Research Journal of Applied Sciences 2 (5): 557-563, 2007

Utilization and Recycling of Industrial Magnesite Refractory Waste Material for Removal of Certain Radionuclides

T.N. Morcos, N.A. Tadrous and E.H. Borai
Hot Laboratories Center, Atomic Energy Authority, Cairo, 13759, Egypt

Abstract: Increased industrialization over the last years in Egypt has resulted in an increased and uncontrolled generation of industrial hazardous waste. The current lack of management of the solid waste in Egypt has created a situation where large parts of the land (especially industrial areas) are covered by un-planned dumps of industrial wastes. Consequently, in the present resaerch, industrial magnesite waste produced in large quantities after production process of magnesium sulfate in Zinc Misr factory, Egypt, was tried to be recycled. Firstly, this material has been characterized applying different analytical techniques such as Infrared spectroscopy (IR), surface analyzer (BET), Particle Size Distribution (PSD), elemental analysis by X-Ray Fluorescence (XRF) and X-Ray Diffraction (XRD). The magnesite material has been used as a source of producing aluminum, chromium and magnesium oxides that has better chemical stability than conventional metal oxides. Secondly, utilization of magnesite material for removal of certain radionuclides was applied. Different factors affecting the removal capability such as pH, contacting time, metal concentration, particle size were systematically investigated. The overall objective was aimed at determining feasible and economic solution to the environmental problems related to re-use of the industrial solid waste for radioacive waste management.

Key words: Industrial waste, magnesite, sorel cement, radionuclides, utilization, XRF

INTRODUCTION

The increasing amounts of wastes and the simultaneous decrease of the waste disposal space as well as the problems associated with the contamination from hazardous and toxic elements are challenges with which the human kind must cope nowadays (Boccacini *et al*., 1996). Therefore, the different types of wastes must be exactly categorized and defined in order to determine the most suitable way for their disposal. According to material science view point, the waste can be described as the material by-products after fabrication and have no further value, especially within affluent developed economies (Gandy, 1993).

On the other hand, using different recycling processes may cause dangerous effects on the surroundings. For example, the environmental concerns associated with incineration emissions and the related problem of the increasing quantities of toxic wastes in waste streams grew rapidly (Gandy, 1993; Gore, 1992). The Berlin based Institute For Ecological Recycling (IFOR) claim that 90% of pollution results from the production process and not in the eventual disposal of products (Koptyziok and Oswald, 1988).

Egypt like several other developing nations, is undergoing unprecedented process of designing and implementing environmental polices and strategies. In 1992, a National Environmental Action Plan (EAP), was formulated by the Egyptian Environmental Affairs Agency (1992). In 1993, a base line report was formulated to assess the overall problem of industrial hazardous waste management in Egypt. Consequently, recommendations for priority actions were identified and the main components of a national hazardous waste system under the provision of law 4/1994 were presented (El-Dars, 1993).

Sorel announced the discovery of an excellent cement formed from the combination of magnesium oxide and magnesium chloride solution (Awwad and Daifallah, 2005). This cement type is known by many different names, such as Sorel, magnesite and magnesite oxychloride cement. This cement has many superior properties to Portland cement. Magnesium oxychloride also bonds very well to a variety of inorganic and organic aggragates, such as saw dust, wood flower, marble flour, sand and gravel giving a cement that has high early strength, conducting and is unaffected by oil grease and paints. The main bonding phases

Corresponding Author: Emad H. Borai, Department of Analytical Chemistry and Environment control, Atomic Energy Authority, Hot Lab Center, 13759, Cairo, Egypt

found in hardened cement pastes are Mg $(OH)_2$, 3 Mg $(OH)_2$. $MgCl_2$. 8 H_2O (3-form) and 5 Mg $(OH)_2$, $MgCl_2$.8 H_2O (5-form).

There are two other known magnesia cements, the first is Magnesium Oxysulfate (MOS), which is the sulfate analogue of magnesium oxychloride and is formed by the combination of magnesium oxide and magnesium sulfate solution. The second is Magnesium Phosphate cement (MAP), formed by the reaction betweem magnsium oxide and a soluble phosphate, such as ammonium phosphate monobasic ($NH_4H_2PO_4$) (Hassan *et al*., 2006).

The main drawback of both magnesium oxychloride and MOS is their unstability in contact with water. Thus different mixtures of MgO-metal bricks were recently developed. Their batch and composition, density, porosity, cold crushing strength, permeability were tested (Jain and Richter, 1993; Ogata *et al*., 1995; Nakanishir *et al*., 1994; Hatafuku *et al*., 1983). The chemical density and porosity of the raw materials (fused magchrome, chrome ore, sinterec Cr_2O_3 powder) were improved.

For agricultural purposes, magnesium sulphate is one of the most important product of Zinc Misr Company (ZMC), in Egypt. The raw material used for this purpose is the exhausted magnesite bricks whose main constituent is MgO (89%). After grinding and leaching of these material in concentrated H_2SO_4 to obtain concentrated solution of $MgSO_4$, the unleached part (magnesite waste material herein after designated as MWM) was taken for further investigation. The chemical and thermal stability of these materials is expected to be very high as they are produced from the refractory bricks of cement kilns that have been subjected to very high temperatures up to 1500°C. Hence the MWM is expected to be appropriate for applications in the nuclear field, especially for removal of radionuclides. One of the most important applications is the pre-concentration of trace Cs^+, Co^{2+} and Eu^{3+} because of their nuclear and radiochemical importance.

MATERIALS AND METHODS

Reagents and solutions: All chemicals and reagents were analytical grade. Hydrochloric, nitric and sulfuric acids were obtained from Merck (Germany). Aqueous solutions prepared with double distilled de-ionized water. Standard stock solutions were quantitatively prepared by dissolving requisite radioactivity level of each radiotracer in a solution containing 5% of nitric acid.

Radioactive tracers and standards: Three different radionuclides were used including ^{134}Cs, ^{60}Co and ^{154}Eu. All these isotopes were prepared by neutron irradiation of an accurate weight of the corresponding nitrate in Egyptian reactor ARE-RR-1 at Inshas (neutron flux ~10^{13}n. $cm^{-2}s^{-1}$). A suitable weight (5-20 mg) was wrapped in an aluminum foil and placed in an irradiation can. The irradiation was performed for 48 h. The produced radionuclides were left to cool for suitable time before being prepared for the required investigations, to allow all short lived unwanted radionuclides to decay.

The irradiated samples were then dissolved in appropriate diluents, evaporated to dryness and redissolved in bi-distilled water. The washing process was repeated to reduce the hydrogen ion concentration.

The γ-activity of the isotopes used was measured using a scintillation probe provided with a NaI (TI) crystal. The scintillation head is connected to a scalar type Rotemeter SR7 made in England. The γ-activity of both solution and solid was measured.

Physico-chemical characterization of magnesite particle: Characterization of the magnesite particle was performed using Quantachrome system model 2.1 (2003), NOVA-type for measuring surface area, the particle diameter and total pore volume.

The particle size distribution of the magnesite particle was determined using lazer diffraction particle size analyzer, Shimadzu, model Sald 2001, Japan.

Infrared spectra were recorded with Bomen Miclson Fourier Transform spectrometer (FT-IR), model MB-157, Canada. The spectra were recorded from 400-4000 cm^{-1} with a resolution at 4 cm^{-1} corresponding to 10 scans per spectrum. The MWM particles were dispersed in KBr and pressed into pellets prior to analysis.

X-ray Diffraction pattern (XRD) was carried out using Shimadzu X-ray diffractometer, model XD-D1(Japan) with a nickel filter and Cu-K_α radiation tube. The scanning speed was 0.02 degree per second.

Elemental analysis of the magnesite material was performed with ultrasensitivety X-ray flourescence technique with X-ray spectrmeter, model PW-2400, Philips.

Adsorption studies: Attempts to find different factors required for sufficient removal of radioactive cesium, cobalt and europium using batch technique were carried out. In batch technique, a particular weight of the magnesite powder was mixed with a certain activity level of each of Cs^+, Co^{2+} and Eu^{3+}.

The influence of critical variables such as shaking time, solution pH and magnesite weight were tested to explore the possibility of using industrial magnesite solid waste material to remove radionuclides.

The mixture is shaked well till equilibrium is reached. The phases were separated and aliquots of the aqueous solution were withdrawn then subjected to radiometric analysis. The uptake percentage of the metal ions between the aqueous phase and the composite powder was calculated using the following formula:

$$\text{Uptake\%} = \frac{C_o - C_e}{C_o} \times 100 \quad (1)$$

Where C_o is the initial metal concentration in the aqueous solution.

C is the final metal concentration at equilibrium in the aqueous solution.

RESULTS AND DISCUSSION

Physico-chemical properties

Surface area and total pore volume: The total surface area of the MWM particle was measured using standard volumetric method by nitrogen adsorption at 273 K and outgas temperature of 150° for 2.0 h and calculated according to muli-point BET equation (Brunouer *et al*., 1937)

$$\frac{p/p^o}{V_a(1-p/p^o)} = \frac{1}{V_m} + \frac{C-1}{C} \times \frac{p/p^o}{V_m} \quad (2)$$

Where P/P^o is the relative pressure

V_a is the amount adsorbed
V_m is the monolyer capacity
C is the constant characteristic of the sample

As shown in Fig. 1, based on the above equation the relationship between relative pressure (P/P^o) and amount adsorbed gives a straight line of slope equal to C-1/C and intercept $1/V_m$.

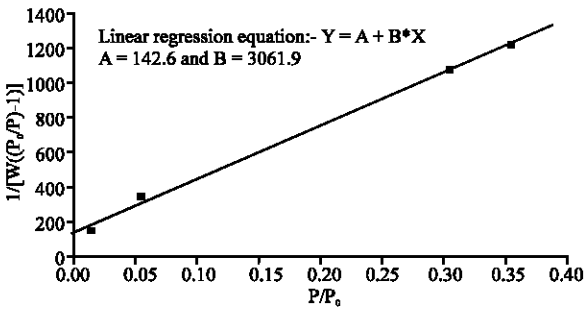

Fig. 1: Relationship between relative pressure (P/P^0) and amount of nitrogen adsorbed

Table 1: Surface area of various industrial solid wastes

Industrial solid waste	Surface area ($m^2\ g^{-1}$)
Blast furnace slag	2.01
Oxygen converter slag	1.5
TV-tube glass	0.54
Flask glass	1.24
Borosilicate glass	0.73
Magnesite material (present work)	1.09

The surface area can be determined from this equation:

$$\text{Surfacearea} = \frac{V_m}{22400} \times N_A \times 16.2 \times 10^{-20} / \text{wt} \quad (3)$$

Where N_A Avogadro's number and wt is the weight of the sample in gram.

Data analysis shows that the total surface area of the magnesite particle is equal to 1.09 $m^2\ g^{-1}$ at relative pressure (P/P^o) of 5.42×10^{-2}. Also the total pore volume is 1.845×10^{-3} Cm^3g^{-1} for pores smaller than 34.5 nm diameter whereas the average pore diameter is 6.79 nm. This small surface area is attributed to non-porous material. The small surface of magnesite solid material (1.09) is expected to be similer to various types of the industrial solid wastes treated at high thermal temperature as presented in Table 1. All of these industrial solid wastes are mainly inorganic metal oxides.

Particle size distribution: The small pore surface area and pore volume demonstrated that almost all portions of magnesite particle are in nano-capillary. This was confirmed by measurement of the average particle diameter and particle size distribution. As shown in Fig. 2, the average particle size (micro meter) (X-axis) was determined at the corresponding values at 50% of the Normalized Particle Amount (NPA%) (Y-axis). It was found that the average particle size distribution at the corresponding value at 50% of NPA was 45 μm.

Infrared spectroscopy: Use of FT-IR spectroscopy led to the spectrum shown in Fig 3. The spectrum confirmed that metal oxide of various types have bands from the metal-O-metal group that can absorb throughout the 200-800 cm^{-1} region. For example, the sulfate ion ($SO4^{-2}$) has its bending band at 590-710 cm^{-1}. Also, the silicates have bands in the 440-570 cm^{-1} region and the Si-O-Si group absorps at 1000-1100 cm^{-1}.

Furthermore, the presence of carboxyl group are usually characterized in the condensed state by a strongly bonded, very broad OH stretching bands at 2800-3100 cm^{-1}. Distinctive shoulders between 2300-2600 cm^{-1} appear regularly in carboxyl group are due to overtones and combinations of the 1300 and 1420 cm^{-1} bands as well as due to interacting of C-O stretch and OH deformation

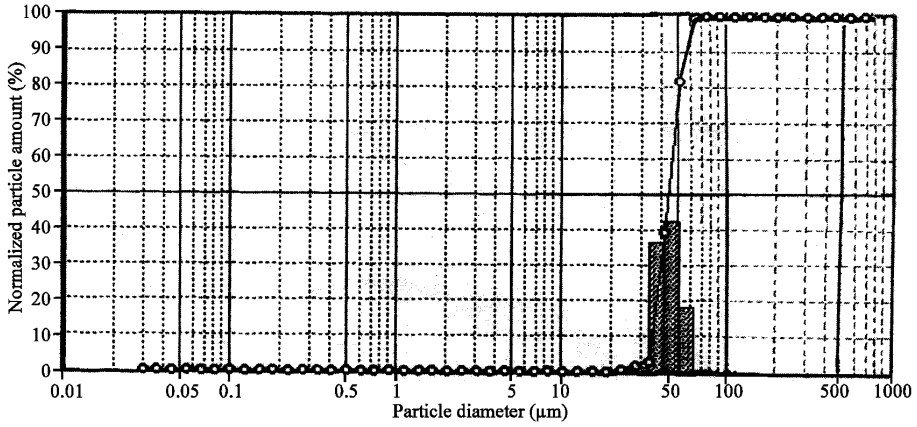

Fig. 2: Particle size distribution of magnesite particles (MWN)

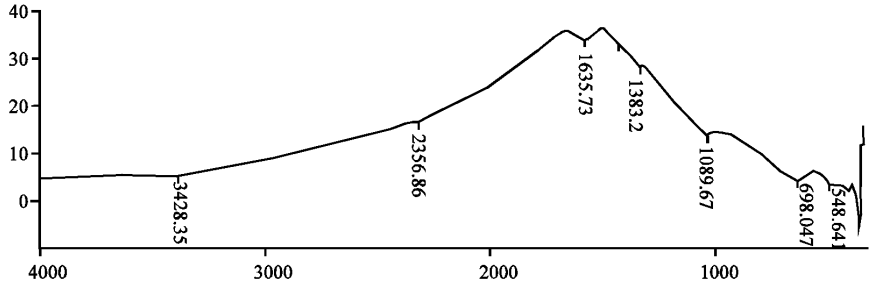

Fig. 3: Infrared spectrum of magnesite waste material particles

Table 2: Elemental analysis of magnesite solid waste by X-ray fluorescence

Metal oxide	MgO	SiO_2	Al_2O_3	Fe_2O_3	CaO	Cr_2O_3	SO_3	K_2O	TiO_2	MnO_2	ZrO_2
Concentration (%)	28.45	4.038	57.34	3.17	0.74	4.405	0.501	0.096	0.581	0.194	0.407

vibrations. Monomeric acids absorb weakly and sharply at 3400-3580 cm^{-1}. Most carboxyl group have a band in the infrared at 1600-1720 cm^{-1} for asymmetric C = O stretch. At high tempreature process, meduim bands at 1280-1380 $cm^{-1}$and strong bands at 1075-1190 cm^{-1}were obtained due to interacting OH deformation in-plane and C-O stretching.

Finally, IR analysis confirmed that MWM particles are mainly contain carboxylate, silicate and sulfate. The main source of carboxylate groups are attributed to the presence of metamorphic marble rocks subjected to high temperature which have a chemical structure like lime stone (calcium carbonate). Also the main source of silicate groups are attributed to the additive sedimentary rocks that mainly contain silicon dioxide (sand and gravel) during cement and bricks production. Sulfate groups are present due to the direct treatment of MgO with concentrated sulfuric acid in ZM company to get magnesium sulfate product.

X-ray flourescence: Visually the MWM has two important fractions. The first white to brownish white colored granular fraction (represent quantitively the main fraction) is mainly Aluminite and Magnesium Oxide. It is commercially known as Gret and contains about 57.34% Al_2O_3 and MgO 28.45% (Table 2). The second fraction is black colored aggregates which are smaller in size and percent compared with first part. This part mainly consists of a mixture of Cr_2O_5 (4.405%) and Fe_2O_3 (3.17%).

As shown in Table 2, the obtained MWM is composed of different types of metal oxides that posses chemical and physical stability which make them useful for application in nuclear technology. As mentioned before this magnesite material waste originates from magnetite-chrome refractory bricks. The chemical composition of different types of magnesite-chrome bricks as declared from SORMA company in Germany is shown in Table 3. Comparing the chemical analysis of the obtained MWM with that type of magnesite-chrome bricks (Table 3), it is obvious that the percentage of MgO decreased sharply and Al_2O_3 is highly increased. That is due to leaching process with H_2S0_4 occurred in Zinc Misr company to

Table 3: Magnesite-chrome and chrome-magnesite bricks (control and supplamentary properties)

	Control properties			Supplementary properties					
	Bulk density	Appearent porosity	Cold crushing strenght	Chemical analysis (%)					
Grade	gr cm^{-3}	(%)	N mm^{-2}	MgO	SiO_2	Al_2O_3	Fe_2O_3	CaO	Cr_2O_3
SÖRK MC 10	2.97	17	68	86	1.8	1.4	2.1	2.2	6
SÖRK MC 10 G	3.00	17	56	83	1.2	3.1	3.4	1.6	6.8
SÖRK MC 12	2.96	17	62	79	1.5	1.3	9.2	2.7	6.4
SÖRK MC 30	3.00	19	43	72	2.1	3.1	4.2	1.9	16
SÖRK MC 40	2.93	21	38	70	2.1	3.6	5.1	1.8	17
SÖRK MC 40 CB	3.07	13	73	71	2.1	3.5	4.9	1.7	16
SÖRK MC 55	3.07	21	28	52	2.5	6.1	7.9	1.3	29
SÖRK MC 60	3.09	21	27	48	2.6	6.6	8.4	1.2	32
SÖRK MC 75	3.12	21	26	37	2.8	8.3	11.1	1.1	39
SÖRK MC 90	3.17	19	40	31	3.2	9.5	12.8	0.8	40
SÖRK M 90 CBS	3.05	13	69	55	1.2	6.7	14.0	0.7	22
SÖRK MK 100	3.03	18	59	61	0.8	6.2	13.2	0.7	17.8
SÖRK MK 20	2.96	17	63	89	1	1.3	3.1	1.8	3.6
SÖRK MK 65	3.08	20	41	48	1.5	7.4	14.0		

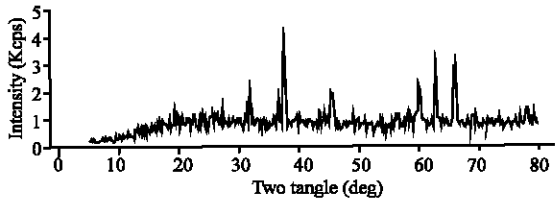

Fig. 4: X-ray diffractogram of magnesite waste material particles

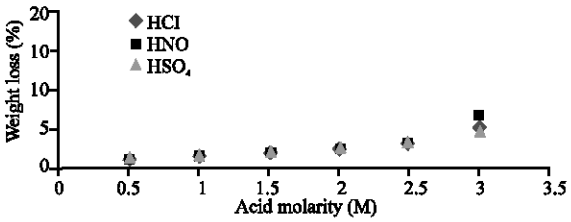

Fig. 5: Srability of magnesite waste material in various inorganic acids

obtain $MgSO_4$ where MgO dissolves in H_2SO_4 and hence results in $MgSO_4$ but Al_2O_3 are not dissolved and then accumulated.

X-ray diffraction: The mineralogical compositions of magnesite waste material through thermal treatment at different temperature, after milling for 30 min. and uniaxial compaction at 83 M Pa, is shown in Fig. 4. The figure shows various types of crystalline phases. X-ray diffractogram shows MWM is mainly Potassium, Aluminum, chromium, magnesium, cholride, silicate similar to potassium, aluminium, chloride silicate appeared in JCPDS-ICDD cards (Hoyle, 1993).

X-ray diffractogram shows not only the main constituting phases but also the distribution pattern of the magnesite paticles. These enables us to observe the microstructure of the magnesite material and by the help of IR and XRF, complete chemical analysis can be obtained.

Equilibria and capacity measurements

Acid stability: As mentioned in the introduction, the main disadvantage of various megnesia materials is its high solubility in acidic water media especially at low pH value. Therefore, the solubility of the magnesite solid waste was tested in various concentrations of different acids such as HCl, HNO_3 and H_2SO_4. As shown in Fig. 5, magnesite waste material is highly stable with insignificant solubility. Up to 3.0 M of each acid, the loss in the weight of the magnesite material due to soaking for one week does not exceed 5.0, 6.0 and 4.0% in HCl, HNO_3 and H_2SO_4, respectively.

Effect of contacting time: The sorption kinetics of Cs^+, Co^{2+} and Eu^{3+}on the MWM containing mixed oxide are studied at different time intervals ranged from 1 to 24 h. As shown in Fig. 6, the equilibrium time for Cs^+, Co^{2+} and Eu^{3+} is reached after 12, 6 and 8 h, respectively.

From the waste management point of view, only 27.2, 84 and 69% from Cs^+, Co^{2+} and Eu^{3+} radionuclides could be decontaminated on magnesite material at 10^{-4} M respective metal ion concentrations.

Ionic radii of the investigated radionuclides are useful for predicting the reaction mechanism inside the crystal structure of the magnesite material. Table 4 presents the ionic radii R_i in angstrom (A°) units for most common Coordination Number (CN) for studying ions Cs^+, Co^{2+} and Eu^{3+} (Shannon, 1974).

Based on the kinetic data and from Table 4, it could be stated that the order of selectivity of the investigated

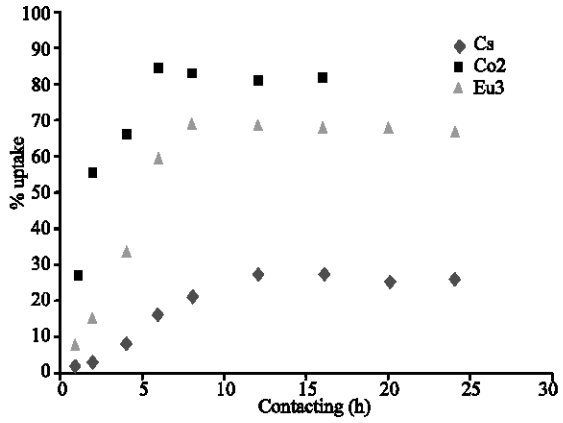

Fig. 6: Effect of contacting time on the uptake percentage of Cs^+, Co^{2+} and Eu^{3+} on MWN at $[M^+] = 10^{-4}$ M/L and v/m = 100

Table 4: Ionic radii of studied Cs^+, Co^{2+} and Eu^{3+} ions

Radionuclide	Coordination Number (CN)	Ionic radius R_i (A°)
Cs^+	6	1.67
	8	1.74
	10	1.81
Co^{2+}	4	0.56
	6	0.65
	8	0.9
Eu^{3+}	6	0.95
	8	1.07

radionuclides was found to be Co>Eu>Cs which may assigned to the high ionic radius of Cs^+ rather than Eu^{3+} and Co^{2+}, which sterically hindred the metal accommodations.

Another important aspect of kinetic order was particularly related to the chemical composition of the MWM which mainly depends on the degree of crystallinity of the magnesite material as well as inter-particle condensation that may arise in the sequence of Co>Eu>Cs and in turn, increasing the wall potentials of the decontaminating pores; i.e., the radionuclides are accommodated inside the pores at different rates.

Effect of pH: Magnesite material is mainly metal oxides, therefore the pH of the solution containing radionuclides plays a determinant role on their removal capability. Accordingly, sufficiently high pH is required for permanent activation of the hydroxide ion on magnesite material which promotes the ion exchange capability. However, sufficiently low pH is necessary to minimize in metal precipitation in the form hydroxides due to metal hydrolysis. As shown in Fig. 7, at pH values less than 5, the precentage uptake is lowered by moving to lower pH. This may be assigned to the decrease in the effeciency of the magnesite powder that acts as a cation exchanger. However, increasing the pH value above 8 led to a considerable reduction in the uptake of the radionuclides that may be attributed to their formation of hydrolyzed species.

Table 5: Effect of volume/weight ratio on the uptake of Cs^+, Co^{2+} and Eu^{3+}on magnesite material

	(%) Uptake		
V m^{-1} (mL g^{-1})	Cs^+	Co^{2+}	Eu^{3+}
25	51	97	84
50	49	96	80
75	46	91	77
100	43	84	69
200	29	67	46

[M] = 10^{-4}, pH = Optimized corresponding values

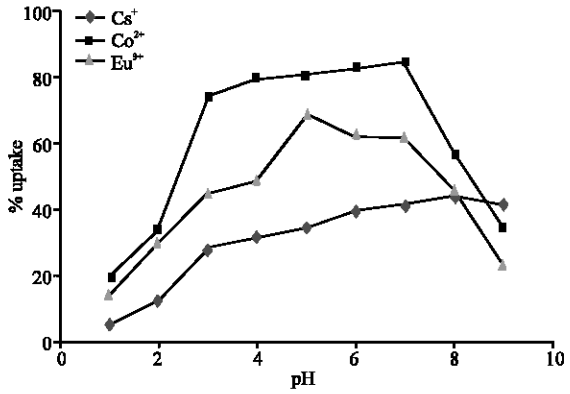

Fig. 7: Effect of pH time on the uptake Cs^+, Co^{2+} and Eu^{3+} on MWN at v m^{-1} = 100 and $[M^+] = 10^{-4}$ M L^{-1}

Figure 7 demonstrated that the maximum uptake percentages were 27.2, 84 and 69% for Cs^+, Co^{2+} and Eu^{3+} at pH 8-7 and 5, respectively. i.e. The optimized percentage uptake values lie in the pH range between 5 and 8.

Under the same conditions, the selectivity order was found to be Co>Eu>Cs. This selectivity order might be explained by increasing their effecive ionic radii rather than exchange process. On the other hand, according to the principle of hard and soft acids, hard acids perfer to bind to hard bases and vice verse. The softness of the cations increase as the ionic radius increases (Shannon, 2005).

Effect of volume/weight ratio: The effect of volume to weight ratio (V m^{-1}) on the uptake of Cs^+, Co^{2+} and Eu^{3+} was studied in the range from 25 to 200 mL mg^{-1}. This is to evaluate the optimum magnesite weight that could be used to achieve a high uptake with a minumum magnesite weight. As shown in Table 5, the uptake increases as V m^{-1} decreases from 200 up to 100. Starting from V m^{-1} equal 100 to 25, the uptake reach to close values. Thus, the optimum V m^{-1} ratio was obtained at 100.

Table 6: Isothermal sorption capacity of Cs^+, Co^{2+} and Eu^{3+} at 10^{-4} M on magnesite material

Metal Ion	V m^{-1} (mL g^{-1})	pH	Capacity (meq g^{-1})
Cs^+	100	8	0.009
Co^{2+}	100	7	0.431
Eu^{3+}	100	5	0.098

Isothermal sorption capacity: The isothermal sorption capacity of the three radionuclides on magnesite material containing various metals oxide were determined using the batch process, by equilibrating 0.05 g of the solid magnesite waste with succsessive additions of 5 mL of aqueous solution containing 10^{-4} M of each radionuclides. The loading capacity of the magnesite material for each metal ion was calculated by mass balance of the difference between the metal ion concentration before and after sorption.

As demonstrated in Table 6, the maximum sorption capacity of magnesite material towards Co^{2+} comparing to Eu^{3+} and Cs^+ confirmed that the selectivity sequence mainly depend on the ionic radius of the metal ion and hence the accommodation rate inside the pores. Furthermore, the high charge-density on the Co^{2+} ion preferentially promotes the binding rate to the hydroxide functional groups of the metal oxides on the magnesite material.

CONCLUSION

Magnesite waste material, MWM, is useful for applications in the field of nuclear technology as it is composed from different metal oxides that posses high chemical, thermal and physical stability.

Based on the morphology of magnesite particle and the ionic radii of the investigated radionuclides, it could be suggested the reaction mechanium is mainly due to pore filling rather than surface adsorption, gradually filling the pores up to pores with a diameter of about 10 nm.

Better performance of this material is attributed to its ability for size exclusion chromatographic behaviors towards divalent cobalt ion, which is added to the normal sorption properties of the oxides.

REFERENCES

Awwad, N.S. and A.A.M. Daifallah, 2005. J. Radioanal. Nucl. Chem., 264: 623-628.

Boccacini, A.R., J. Janczak, D.M.R. Taplin, and M. Koepf, 1996. Environ. Tech., 17: 1193-1203.

Brunouer, S., P.H. Emmett and B. Teller, 1937. J. Am. Chem. Soc., 59: 1553.

Egyptian Environmental Affairs Agency (EEAA), 1992. The Environmental Action Plan (EAP), Cabinet of Ministers, Egypt.

El-Dars F., 1993. Industrial hazardous waste management in Egypt. Baseline Study, The Technical Cooperation Office for the Environment (TCOE) Egyptian Environmental Affairs Agency (EEAA).

Gandy, M. 1993. Recycling and waste, exploration of contemporary environmental policy-avebury studies in green research series, Ashgate Publishing Limited, London.

Gore, A., 1992. Plume, New York.

Hassan, S.S.M., N.S. Awwad, A.H. Aboterika and A., 2006. J. Radioanal. Nucl. Chem., 269: 135-140.

Hatafuku, H., S. Takahashi, T. Sasaki and H. Ichinoho, 1983. J. Magnetism and Magnetic Mater., 31-34: 847-848.

Hoyle, S., 1993. Penn State Univ., University Park, PA, USA, ICDD Grant-in-aid.

Jain, M.K. and T. Richter, 1993. Unitecr '93 congress. Referactories for the new world economy. Proc. Conf. Sao Paulo, 3: 1039-1049.

Koptyziok, N. and R. Oswald, 1988. In Ifor Abfall Vermieden, Fischer taschenbuch Verlag, Frankfurt am Main, pp: 69-74.

Nakanishi, T., R. Nakagawa, I. Kusunose, M. Yamasaki and M. Koyama, 1994. Refractories, 46: 432-433.

Ogata, M., T. Hisamoto, K. Saito and T. Yamamura, 1995. Refractories, 47: 73-81.

Shannon, R.D., 2005. Acta Crystallogr., A32, 751, 1974. Handbook of Chemistry and Physics, CRC.

Tanahashi, N., A. Takeuchi and K. Tanaka, 2001. J. Energy Resources Tech., 123: 76-80.